Experimental Characterization of the Threshold- and Fatigue Crack Growth Behaviour Regarding Negative Stress Ratios

Viktor Kloster [1,a] , Hans Albert Richard [1,b] and Gunter Kullmer [1,c]

[1] Institute of Applied Mechanics, Faculty of Mechanical Engineering, Universität Paderborn,

Pohlweg 47-49, 33098 Paderborn, Germany

[a] kloster@fam.upb.de, [b] richard@fam.upb.de, [c] kullmer@fam.upb.de

Abstract. This paper focuses on the fracture mechanical characterization of materials for varying loading conditions. Particularly the influence of mean stress and threshold behaviour are analyzed for negative stress ratios. Therefore novel testing device concepts for backlash-free load application are introduced. Applying the developed testing devices a material typically used in chassis technology is experimentally characterized for different stress ratios and load levels. The determined fatigue crack growth curves with the corresponding threshold values are quantified and visualized in diagrams. Furthermore several theoretical concepts for the description of the crack growth curves including the mean stress effect and the threshold behaviour are discussed.

Introduction

Within the damage tolerant component design the evaluation of the fatigue crack growth and particularly the determination of the residual service life of components represent fundamental aspects [1]. The reliable estimation of the residual service life demands an accurate fatigue crack growth characterization of the used materials for different stress ratios and the description of these mean stress dependent crack growth data with theoretical concepts. These concepts have to be validated experimentally. Therefore novel testing device concepts for a backlash-free load application are introduced within this paper. Furthermore a material typically used in chassis technology is experimentally characterized. With the aid of the experimental findings the mean stress effect and several theoretical concepts are analyzed und validated.

Testing device concepts for backlash-free load application

For the experimental characterization of fatigue crack growth the standard ASTM E 647-8 [2] recommends three different specimen types (CT-, ESET- and MT-specimen). However, neither the CT-specimen nor the ESET-specimen in combination with the standardized testing devices is applicable for experimental investigations with negative stress ratios due to the load application with backlash. Merely the MT-specimen is suitable for the realization of a backlash-free load application and stable testing control. Though, the MT-specimen has an essential disadvantage concerning the measurement of the crack length. Using optical measurement techniques or measuring films it is required to measure all four crack tip positions to quantify the crack length exactly. The measurement of only two crack tip positions doesn't enable the identification of the non-uniform crack front propagation. The application of the potential drop method to the MT-specimen provides solely the measurement of an integral value of the crack surface extension without any separate information about the respective propagation of the both crack fronts. Taking these aspects into account clear and automated testing procedures using the MT-specimen are unrealizable. To ensure a backlash-free load application and the usage of the potential drop method with different specimen types, the standard ISO 12108 [3] recommends the clamped SENT-specimen and the eight point single edge notch bending (SENB8) specimen.

In several publications [4,5] the SENT-specimen is used for fracture mechanical examinations at negative stress ratios. Other authors use modified CT-Specimen for that kind of investigations. *Beretta* et al. [6] use a CT-Specimen with the adoption of threaded rigid pins for the load application whereas *Zhao* et al. [7] use a tight tolerance or a press-fit between the loading pin and the hole in the specimen.

The realization of the backlash-free load application by clamping or due to the usage of the press-fit constrains the rotary degrees of freedom. Consequently the standardized stress intensity factor functions (*K*-calibration) are limited valid for this purpose. The subsequently explained novel testing devices counteract this restriction by the application of special slide bearings and due to the numerical determination of the effective *K*-calibration. The developed testing device concepts are based on the standard CT-specimen and the SENB-specimen.
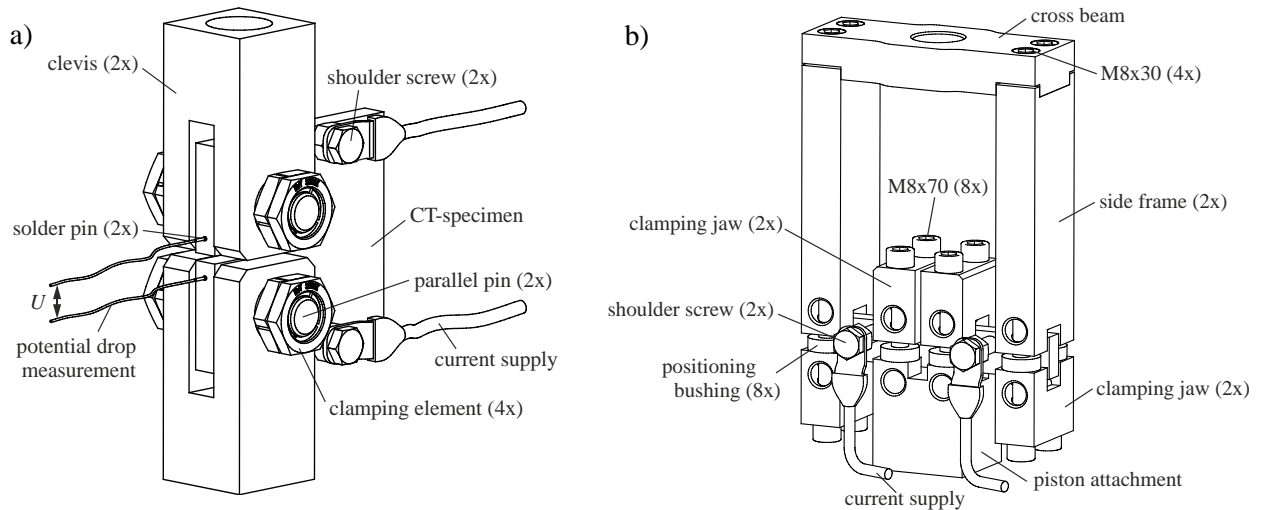

Fig. 1. Testing device concepts for backlash-free load application in the a) CT- and b) 4PB-specimen

The backlash-free load application with the novel CT-specimen testing device concept, see Fig. 1a, is realized by the implementation of slide bearings and special clamping elements. The bearing clearance between the specimen holes and the loadings pins is eliminated by the choice of a transition-fit. Due to the transition-fit and the PTFE-Pb sliding coat at the running layer of the bearing the friction is reduced and no significant rotary constraints exist. In addition to the reduction of the frictional resistance the PTFE-Pb sliding coat isolates electrically the specimen against the testing device. The clamping elements consist of two screwed conical clamping sleeves and enable the backlash-free join connection between the clevis and the loading pin by interlocking the clamping system [8].

For the examination of the sensitivity of the fatigue crack growth data to the specimen geometry especially for negative stress ratios and for the validation of the transferability of the determined fatigue crack growth curves although the 4PB-specimen testing device was developed based on the SENB-specimen, see Fig. 1b. The four-point-bending testing device enables the backlash-free load application based on the principle of the standardized SENB8-specimen [3]. Thereby the 4PB-specimen is arrested between eight roller bearings and defined clamped with tensioning screws. During the cyclic loading and depending on the loading direction only four of the eight roller bearings are loaded simultaneously. Resulting forces and undesired bending moments due to the pretensioning of the clamping bolts and the friction are reproducibly adjusted by using a torque controlled pretensioning technique. Furthermore the influence of the pretensioning is considered within the numerical determination of the stress intensity factor function (*K*-calibration). The electrical isolation between 4PB-specimen and testing device is realized by the both-sided adjustment of the specimen with positioning bushings and the usage of ceramic roller bearings [8].

The functionality of the developed testing devices regarding the backlash-free load application is shown by the force-displacement-relationship in Fig. 2.
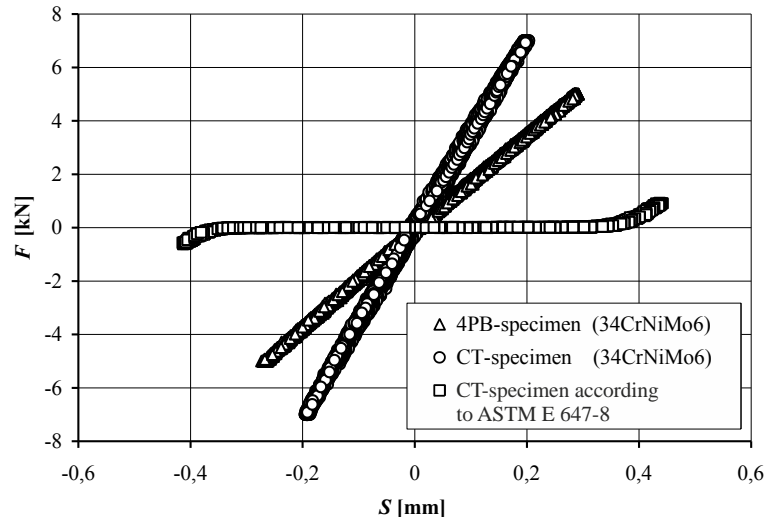
Fig.2. Force-displacement-relationship of the testing devices for the zero crossing of the loading force

During the zero crossing of the loading force the standardized CT-specimen testing device [2] show a significant backlash of approximately 0,6 mm. The introduced novel testing devices show no measurably backlash.

Experimental study of the mean stress effect
The following section presents the investigated material, the testing procedure and finally the results of the fatigue crack growth examinations.

Investigated Material. For the experimental examination of the R-ratio influence the CrNiMo alloyed steel 34CrNiMo6 is used. This quenched and tempered steel with the chemical composition given in Table 1 is primary used in machinery and vehicle construction for components with especially high stress requirements.

**Table 1.** Main alloying elements of the tempered steel 34CrNiMo6 [9]

chemical composition, mass fraction in [%]							
C	Si	Mn	P	S	Cr	Ni	Mo
$0,3 - 0,38$	$\leq 0,4$	$0,5 - 0,8$	$\leq 0,025$	$\leq 0,035$	$1,3 - 1,7$	$1,3 - 1,7$	$0,15 - 0,3$
0,35	0,27	0,56	0,009	0,001	1,57	1,63	0,21

For the present heat treatment conditions, characterized by the annealing at 860°C for 9 hours and subsequent quenching in oil, combined with the tempering at 620°C for the period of 13 hours and cooling down at air conditions, the used steel feature mechanical characteristics according to Table 2.

Table 2. Mechanical characteristics of the tempered steel 34CrNiMo6 [9]

material	E [MPa]	$R_{p0,2}$ [MPa]	R_m [MPa]	A [%]	hardness [HB]
34CrNiMo6	210000	626	819	19,3	253

Experimental setup and testing procedure. The fatigue crack growth experiments are done with the aid of the previously explained testing devices and the respective specimens. The geometric dimensions of the specimens result from the characteristic specimen width $w = 72$ mm for the CT-specimen [2] and $w = 20$ mm for the 4PB-specimen [3] and the consistent specimen thickness $B = 10$ mm. The experimental investigations are carried out at the laboratory of the Institute of Applied Mechanics with a servo-hydraulic tension-compression testing machine "SCHENCK Hydropuls® PSA 100" using the [FAM]Control [10] control system. All investigations are performed at an ambient temperature of 20°C using a testing frequency of 30 respectively 40 Hz. The determination of the fatigue crack growth curves and the corresponding threshold values is done with two different testing procedures, see Fig. 3.
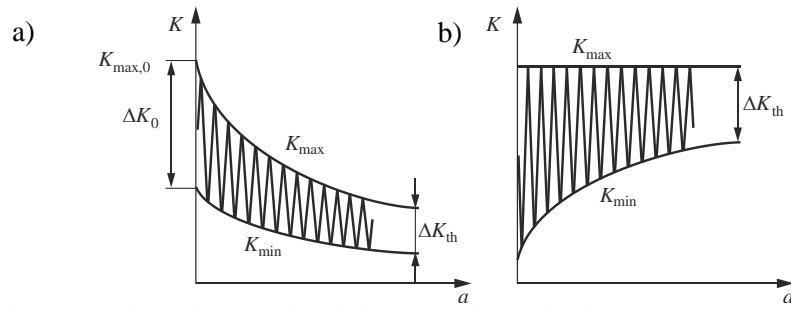
Fig. 3. Testing procedures for the threshold value determination a) R = const., b) K_{max} = const.

Using the R = const. testing procedure, Fig. 3a, for the threshold value determination the cyclic stress intensity range is reduced exponentially until the stoppage of the crack growth. Within the realized investigations this testing procedure is applied for the R-ratios of R = 0,5; 0,1; 0; -0,3; -0,7 and R = -1. The testing procedure with K_{max} = const., Fig. 3b, is also characterized by the exponential reduction of the stress intensity range in which the minimal stress intensity K_{min} is continuously increased. The threshold determination with K_{max} = const. conditions is carried out for the K_{max}-levels of K_{max} = 40; 30; 24 and 15MPam$^{1/2}$.

Fatigue crack growth curves for R = const. and K_{max} = const. The determined fatigue crack growth curves using the R = const. testing procedure are visualized in Fig. 4. The presented fatigue crack growth curves show a pronounced influence of the applied stress ratio on the crack growth rate and the threshold value. The fatigue crack growth rate increases with increasing R-ratio. Consequently the threshold value and the cyclic fracture toughness decreases. Furthermore it can be observed that the mean stress effect is more pronounced in the threshold region than in the *Paris*-regime. This phenomenon can be explained by the higher sensitivity of the crack growth rate against the applied stress ratio especially in the threshold-regime due to the influence and the interaction of different factors [11].

The comparison of the specimen specific fatigue crack growth rate curves shows some differences for the threshold-regime. These deviations can be quantified with approximately 10%. However, the overall examination of the curves shows a good agreement between the both specimen types. The slight differences of the curves in the threshold region can be explained by constraint effects [12,13,14] resulting from different specimen geometry or rather the specimen size.
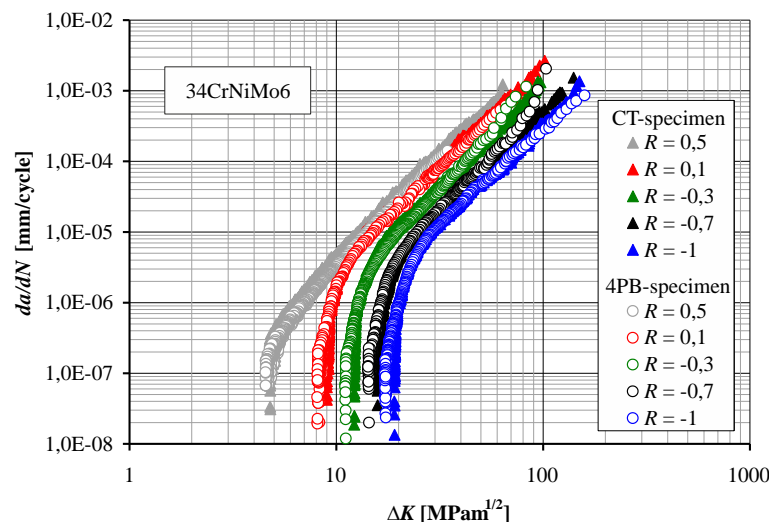
Fig. 4. Comparison of the fatigue crack growth curves determined with novel CT-/4PB-specimen

The experimental fatigue crack growth characterization based on the testing procedure with K_{max} = const. enables due to the varying stress ratio the investigation of a wide range of loading conditions. Therefore fatigue crack growth rates for different stress ratios are determined. Furthermore this testing procedure enables the determination of threshold values for very high R-ratios. The determined fatigue crack growth curves for the K_{max}-levels 40; 24 and 15MPam$^{1/2}$ are

visualized in Fig. 5 combined with $R = $ const. fatigue crack growth curves. For the stress ratio range of $-1 \leq R \leq 0$ the measured crack growth rate only depends on the applied K_{max}-level. In this range the fatigue crack growth rate remain nearly constant without any effect of the stress ratio because only the positive amplitude of the applied load contributes to the crack opening. For stress ratios above $R \approx 0$ the influence of the R-ratio becomes more significant. The crack growth rate decreases with increasing stress ratio until the threshold value is reached.
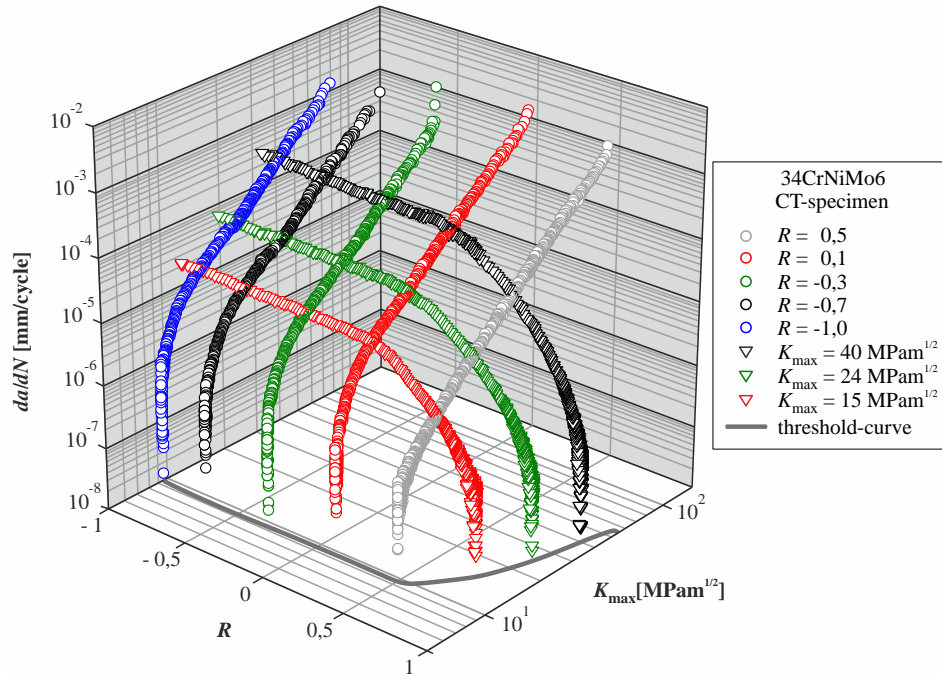
Fig. 5. 3D-representation of the fatigue crack growth rate curves for the material 34CrNiMo6

The determined and analyzed fatigue crack growth curves for the tempered steel 34CrNiMo6 are depending on the applied cyclic stress intensity ΔK as well as on the applied maximum load level K_{max}. Both parameters are coupled by the stress ratio $R = 1 - \Delta K / K_{max}$. The correlation of these parameters is shown in Fig. 5 with aid of the 3D-diagram [5]. The combined illustration of the measured fatigue crack growth rate curves from both mentioned testing procedures clarifies once more the influence of the mean stress on the fatigue crack growth. Additionally to the crack growth data the 3D-diagramm shows the corresponding threshold-curve. This curve represents the threshold behaviour of the investigated steel.

Threshold behaviour. The threshold value represents a significant material characteristic for the evaluation of the fatigue crack growth. The experimentally determined threshold values for the investigated steel are quantified in Fig. 6.
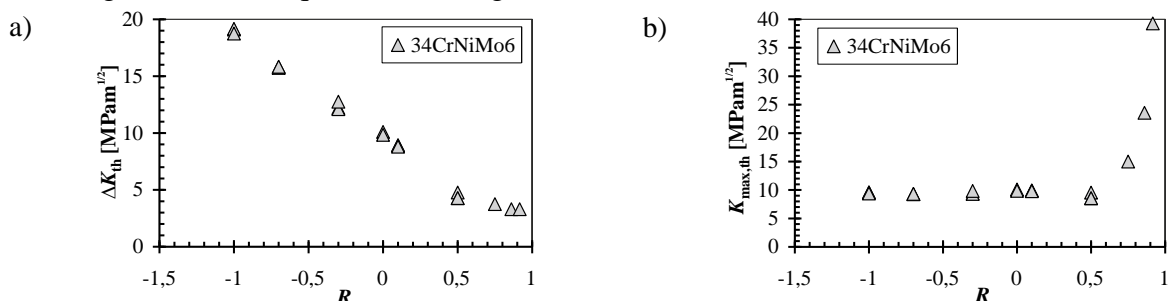

Fig. 6. Threshold values a) ΔK_{th} and b) $K_{max,th}$ as a function of the R-ratio

In these diagrams the measured threshold values are plotted in dependence of the R-ratio. The overall results show a relatively low scatter of the measured thresholds and a significant influence of the applied stress ratio. Within the range $-1 \leq R \leq 0,5$ a linear correlation between the threshold value ΔK_{th} and the R-ratio can be identified. For high stress ratios $R > 0,5$ the slope

of the best-fit line is decreasing, because the intrinsic threshold value ΔK^{*}_{th} [15,16] of the material is nearly reached. The exemplified linear relationship up to the stress ratio of $R \approx 0{,}5$ is also transferable to the distribution of the maximum component $K_{max,th}$ of the threshold. The maximum component of the threshold $K_{max,th}$ remains nearly constant up to the stress ratio of $R \approx 0{,}5$. Due to the preservation of the intrinsic threshold value ΔK^{*}_{th} the maximum of the threshold $K_{max,th}$ increases significantly for higher R-ratios. Basically it can be observed that the threshold behaviour of the tempered steel 34CrNiMo6 is controlled by ΔK for stress ratios above $R = 0{,}5$ and by K_{max} for $R < 0{,}5$.

Validation of theoretical concepts and functions

The influence of the mean stress on the fatigue crack growth rate can be described with theoretical concepts. Several empirical concepts developed by *Elber* [17], *Schijve* [18] and *Kurihara* et al. [19] consider the mean stress effect by the determination of the crack opening function $U = \Delta K_{eff}/\Delta K$. The crack opening function primary characterizes the effective stress intensity ΔK_{eff}. The effective stress intensity is independent of the stress ratio and describes the part of the loading cycle when the crack is opened without any crack closure effects [20] which contributes to the crack propagation. The *Walker* approach $\Delta K_{Walker} = \Delta K/(1-R)^{1-\gamma}$ [21,22] proposes an effective stress intensity range at $R = 0$. Thus the crack will not propagate for the compressive part of the loading cycle and the crack growth is controlled by K_{max} for $R \leq 0$ and by ΔK if $R > 0$. The comparison of the explained concepts with the experimentally determined threshold values for the tempered steel 34CrNiMo6 is visualized in Fig. 7.
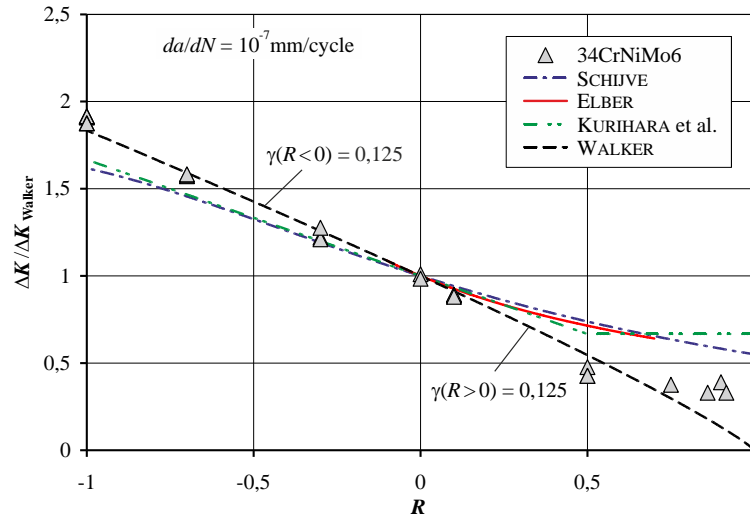

Fig. 7. Validation of the different concepts for the description of the mean stress effect

The verification shows a good correlation between the measured threshold values and the *Walker* approach. Merely the threshold values for $R > 0{,}5$ are approximated inaccurately. The mentioned empirical concepts show a more pronounced deviation between the predicted and the measured threshold values. The mismatch can be constituted with the empirical derivation of these concepts based on crack growth data primarily characterizing the *Paris*-regime and on differing materials. The main objective of the theoretical concepts is to reproduce and predict the fatigue crack growth data for a wide range of stress ratios based on the calibration of these using a minimal number of experimentally determined fatigue crack growth curves and threshold values. The description of the threshold behaviour depending on the crack closure and the stress ratio is given by the following NASGRO-threshold-expression [23]:

$$\Delta K_{I,th}(R,a) = \frac{\Delta K_{th,0} \cdot \sqrt{\dfrac{a}{a + a_0}}}{\left[\dfrac{1 - f_{op}(R)}{(1 - A_0) \cdot (1 - R)}\right]^{(1 + C_{th} \cdot R)}} \cdot \tag{1}$$

To calibrate the description of the threshold behaviour the NASGRO-threshold-equation is fitted to three measured threshold values, see Fig. 8a. The calculated threshold-curve using the determined Parameters is illustrated in Fig. 8b. The calculated curve shows a good agreement between the predicted and the measured threshold values.
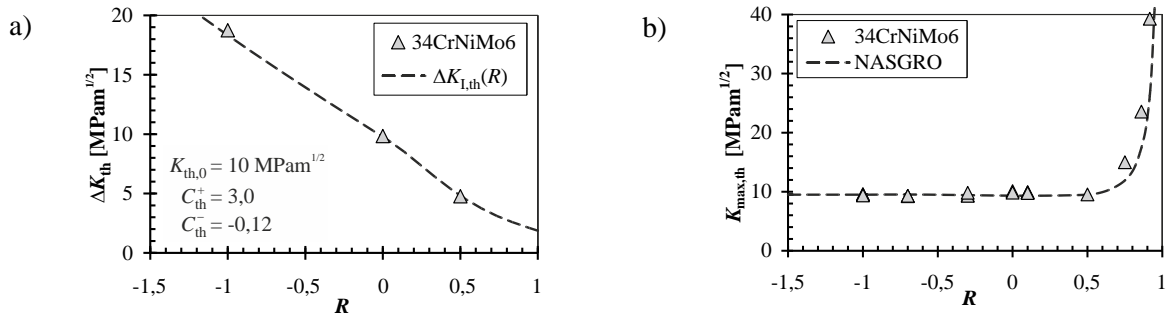

Fig. 8. Description of the Threshold behaviour: a) Threshold-curve fitting and b) Threshold-curve calculated with NASGRO-threshold-equation

Using the calibrated threshold-equation the fatigue crack growth data $da/dN = f(\Delta K, R)$ can be calculated for different loading conditions with the so-called *Forman*/*Mettu* or NASGRO equation [24,23]:

$$\frac{da}{dN} = C_{FM}\left[\left(\frac{1-f_{op}(R)}{1-R}\right)\Delta K\right]^{n_{FM}} \cdot \frac{\left(1-\dfrac{\Delta K_{I,th}(R,a)}{\Delta K_I}\right)^p}{\left(1-\dfrac{K_{I,max}}{K_{IC}}\right)^q}. \tag{2}$$

In this equation C_{FM}, n_{FM}, p and q are empirical constants. R is the stress ratio, $\Delta K_{I,th}$ is the threshold stress intensity range (Eq. 1), $K_{I,max}$ is the maximum applied stress intensity and K_{IC} is the fracture toughness. Fitting the mentioned constants and parameters using the measured fatigue crack growth curve for $R = -1$ further fatigue crack growth curves for the R-ratios $R = 0,1$ and $R = -0,3$ are calculated and compared with experimental data in Fig. 9.
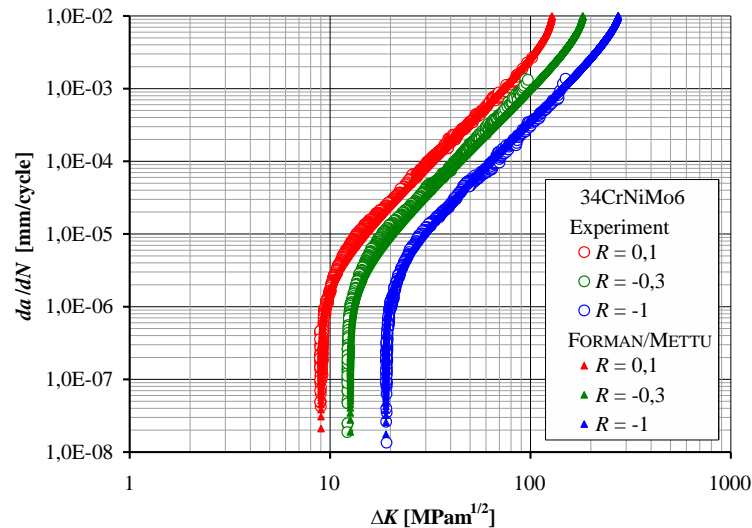
Fig. 9. Comparison between experimental crack growth data and Forman/Mettu-calculation

The comparison between the measured and calculated curves shows a nearly coincident curve progression. The NASGRO equation enables an accurate calculation of the crack growth data for the threshold range as well as for the rest of the curve. Concerning these results it can be concluded, that it is possible to ensure an exact prediction of the fatigue crack growth data by calibration the concepts using only three experimentally determined threshold values and one crack growth curve for a negative stress ratio.

Summary

For a complete characterization of the fatigue crack growth especially regarding negative stress ratios novel testing devices have been developed. The testing devices enable the backlash-free load application. Using these testing devices the fatigue crack growth for the tempered steel 34CrNiMo6 is analyzed for different R-ratios and K_{max}-levels. The determined fatigue crack growth curves show a significant influence of the applied stress ratio on the crack growth rate and the threshold value. The mean stress effect can be described with several theoretical concepts. These have to be calibrated using crack growth curves particularly for negative stress ratios. The combination of the determined fatigue crack growth curves and the theoretical concepts ensure a reliable service life estimation of cyclically loaded pre-cracked components and structures.

References

[1] SANDER, M.: Sicherheit und Betriebsfestigkeit von Maschinen und Anlagen. Springer-Verlag, Berlin, 2008.

[2] ASTM: Annual Book of ASTM Standards. Section 3: Metals Test Methods and Analytical Procedures, Volume 03.01, Metals – Mechanical Testing; Elevated and Low-Temperature Tests; Metallography, 2008.

[3] ISO 12108:2002: Metallic materials – Fatigue testing – Fatigue crack growth method. International Organization for Standardization, 2002.

[4] KUJAWSKI, D.; SREE, P. C. R.: Generation and analysis of FCG data using a single specimen and K_{max}-ΔK testing matrix. In: International Journal of Fatigue, Vol. 31, 2009, pp. 1638-1647.

[5] STEINBOCK, J.: Einfluss unterschiedlicher mechanischer Belastungen auf das Ermüdungsrisswachstum in Stählen und Aluminiumlegierungen. Dissertation, Universität der Bundeswehr München, München, 2008.

[6] CARBONI, M.; BERETTA, S.; MADIA, M.: Analysis of crack growth at R = −1 under variable amplitude loading on a steel for railway axles. In: ASTM STP, Volume 1508, 2009, pp. 574-591.

[7] ZHAO, T.; ZHANG, J.; JIANG, Y.: A study of fatigue crack growth of 7075-T651 aluminum alloy. In: International Journal of Fatigue, Volume 30, 2008, pp. 1169-1180.

[8] KLOSTER, V.; RICHARD, H. A.; KULLMER, G.: Experimentelle Untersuchungen des Mittelspannungseinflusses auf die Ermüdungsrissausbreitung. In: DVM-Bericht 244, Deutscher Verband für Materialforschung und –prüfung e.V., Berlin, 2012, S. 121-130.

[9] INSPECTION CERTIFICATE: Abnahmeprüfzeugnis 3.1 nach DIN EN 10204, Nr. S 3409, Chargen-Nr. GP 78498, Schmiedewerke Gröditz, Gröditz, 2010.

[10] SANDER, M.; RICHARD, H. A.: Automatisierte Ermüdungsrissausbreitungsversuche. In: Materialprüfung, 46, 2004, S 22-26.

[11] LIAW, P. K.; LEA, T. R.; LONGSDON, W.A.: Near-threshold fatigue crack growth behavior in metals. In: Acta Metallurgica 31 (10), 1983, pp. 1581-1587.

[12] HUTAŘ, P.; SEITL, S.; KNÉSL, Z.: Effect of constraint on fatigue crack propagation near threshold in medium carbon steel. In: Computational Materials Science, Vol. 37, 2006, pp. 51-57.

[13] SEITL, S.; HUTAŘ, P.; KNÉSL, Z.: Sensitivity of Fatigue Crack Growth Data to Specimen Geometry. In: Key Engineering Materials, Vols. 385-387, 2008, pp. 557-560.

[14] VARFOLOMEEV, I.; LUKE, M.; BURDACK, M.: Effect of specimen geometry on fatigue crack growth rates for railway axle material EA4T. In: Engineering Fracture Mechanics, Vol. 78, 2011, pp. 742-753.

[15] SCHINDLER, H. J.: Charakterisierung und Abschätzung des Ermüdungsrissverhaltens im Bereich des Schwellenwerts. In: DVM-Bericht 231, Deutscher Verband für Materialforschung und –prüfung e.V., Berlin, 1999, S. 121-130.

[16] DÖKER, H.: Fatigue crack growth thresholds: implications, determination and data evaluation. In: International Journal of Fatigue, Volume 19, 1997, pp. 145-149.

[17] ELBER, W.: Fatigue crack closure under cyclic tension. In: Engineering Fracture Mechanics, Vol. 2, 1970, pp. 37-45.

[18] SCHIJVE, J.: Some formulas for the crack opening stress level. In: Engineering Fracture Mechanics, Vol. 14, 1986, pp. 461-465.

[19] KURIHARA, M.; KATOH, A.; KAWAHARA, M.: Analysis of Fatigue Crack Growth Rates Under a Wide Range of Stress Ratios. In: Journal of Pressure Vessel Technology, Vol. 108, 1986, pp. 209-214.

[20] SURESH, S.: Fatigue of Materials. Second Edition, Cambridge University Press, Cambridge, 1998.

[21] WALKER, K.: The effect of stress ratio during crack propagation and fatigue for 2024-T3 and 7075-T6 aluminum. In: Rosenfeld, M. S. (ed.): Effect of environment and Complex Load History on Fatigue Life, ASTM STP 462. ASTM, Philadelphia, 1970, pp. 1-14.

[22] MANN, T.: The influence of mean stress on fatigue crack propagation in aluminum alloys. In: International Journal of Fatigue, Vol. 29, 2007, pp. 1393-1401.

[23] NASA: Fatigue crack growth computer program „NASGRO". Version 3.0 – Reference Manual. NASA, Lyndon B Johnson Space Center, Texas, 2000.

[24] FORMAN, R. G.; METTU, S. R.: Behavior of Surface and Corner cracks subjected to Tensile and Bending Loads in Ti-6Al-4V Alloy. In: Ernst, H. A., Saxena A., McDowell D. L. (Eds.): Fracture mechanics. 22nd Symposium, Volume I, ASTM STP 1131. ASTM, Philadelphia, 1992, pp. 519-546.